World Journal of Engineering Research and Technology
WJERT
www.wjert.org
SJIF Impact Factor: 5.924

EFFECT OF ACTIVATION ENERGY ON CONVECTIVE HEAT AND MASS TRANSFER FLOW OF DISSIPATIVE NANOFLUID IN VERTICAL CHANNEL WITH BROWNIAN MOTION AND THERMOPHORESIS IN THE PRESENCE OF IRREGULAR HEAT SOURCES

Dr. M. Nagasasikala*

Lecturer in Mathematics, Government Degree College (A), Anantapuramu – 515 003, A.P., India.

Article Received on 10/12/2022 **Article Revised on 30/12/2022** **Article Accepted on 20/01/2023**

***Corresponding Author**
Dr. M. Nagasasikala
Lecturer in Mathematics, Government Degree College (A), Anantapuramu – 515 003, A.P., India.

ABSTRACT

An attempt has been made to analyze the impact of dissipation and activation energy on convection heat transfer flow of a nanofluid in vertical channel. Brownian motion of thermophoresis in the presence of heat sources. By employing Runge-Kutta shooting technique the non linear governing equations have been solved. The velocity, the temperature and nano particle concentration have been discussion for different parametric variation. It is found that an increase is Eckert number (Ec) increase in velocity and temperature smaller Concentration. Cf, Sh grow, Nu decay with Sc. Cf, Nu grow with Ec at. $\eta = \pm 1$. Temperature and nanoparticle concentration grow and velocity augments with increase in E1.Increase in δ grows the velocity, temperature and reduces nanoparticle concentration.

KEYWORDS: Dissipation, Activation energy, Brownian motion, thermophoresis, Heat Sources, Vertical channel, Nanofluid.

1. INTRODUCTION

Viscous dissipation plays a significant role in natural convection in various devices that are subjected to large variations of gravitational force or that operate at high rotational speeds as

published by Gebhart and Mollendorf.[9] analyzed the effect of viscous dissipation in external natural convection considering exponential variation of wall temperature through a similarity solution. Viscous dissipation, a partially irreversible process, which happens due to shear forces transforming heat into fluid flow, has been studied by many researchers for different geometries. Barletta and Pulvirenti.[4] studied the forced convection with slug flow and viscous dissipation in a rectangular duct. Vajravelu and Hadjinicolaou.[22] analysed the heat transfer in a viscous fluid over a stretching sheet with viscous dissipation and internal heat generation.

Heat-transfer enhancement in engineering and industrial systems is one of the hottest topics in research today. With the growing demand for efficient cooling systems, more effective coolants are required to keep the temperature of heat-generating engines and engineering devices such as electronic components below safe limits. In recent time, the use of nanofluids has provided an innovative technique to enhance heat transfer. Nanotechnology has been widely used in engineering and industry, since nanometer-sized materials possess unique physical and chemical properties. The addition of nanoscale particles into the conventional fluids like water, engine oil, ethylene glycol, etc., is known as nanofluid and was firstly introduced by Choi.[1] Moreover, the effective thermal conductivity of conventional fluids increases remarkably with the addition of metallic nanoparticles with high thermal conductivity. Nanofluids may be considered as single phase flows in low solid concentration because of very small sized solid particles. There are many experimental and theoretical studies on the flow of nanofluids in different geometries (Abo-Eldahab.[1] Abu-Nada,[2] Al-Nimir,[3] Buongiorno,[5] Cebeci et al,[6] Choi et al,[8] Gill et al,[10] Greif.[11]). A numerical study of buoyancy-driven flow and heat transfer of an alumina (Al_2O_3)–water-based nanofluid in a rectangular cavity was done by Hwang etal.[12] The nanofluid in the enclosure was assumed to be in a single phase. It was found that for any given Grashof number, the average Nusselt number increased with the solid volume concentration parameter. Nield and Kuznetsov.[11] investigated numerically the Cheng–Minkowycz problem for a natural convective boundary-layer flow in a porous medium saturated by a nanofluid. Oztop and Abu-Nada.[19] considered natural convection in partially heated enclosures having different aspect ratios and filled with a nanofluid. They found that the heat transfer was more pronounced at low aspect ratios and high volume fractions of nanoparticles.

Meanwhile, in the nanofluids flows, the improvement of the heat transfer properties causes a reduction in entropy generation. The foundation of knowledge of entropy production goes back to Clausius and Kelvin's studies on the irreversible aspects of the second law of thermodynamics. Since then the theories based on these foundations have rapidly developed, see.[15,16] However, the entropy production resulting from heat and mass transfer coupled with viscous dissipation in nanofluids has remained untreated by classical thermodynamics, which motivates many researchers to conduct analyses of fundamental and applied engineering problems based on second law analysis with respect to nanofluid. Based on the concept of efficient energy use and the minimal entropy generation principle, optimal designs of thermodynamic systems have been widely proposed base on the second law of thermodynamics (Olanrewaju and Makinde.[17]). It is possible to improve the efficiency and overall performance of all kinds of flows and thermal systems through entropy minimisation techniques. The analysis of energy utilisation and entropy generation has become one of the primary objectives in designing a thermal system. This has become the main concern in many fields such as heat exchangers, turbo machinery, electronic cooling, porous media and combustion. Several studies have thoroughly dealt with conventional fluid flow irreversibility due to viscous effect and heat transfer by conduction (Ostrach.[18], Oztop and Abu-Nada.[19] Tiwari and Das.[21] Wang and Mujumdar.[23]). Makinde et al.[14] performed numerous investigations to calculate entropy production and irreversibility due to flow and heat transfer of nanofluids over a moving flat surface. They found that the entropy generation in the flow system can be minimised by appropriate combination of parameter values together with nanoparticles volume fraction. Recently, Satya Narayana and Ramakrishna.[20] discussed the effect t of Brownian motion and thermophoresis, activation energy on hydromagnetic convective heat transfer flow of nanofluid in a vertical channel.

In the present study, we analyse the combined effects of activation energy, dissipation, thermophoresis, Brownian motion, and variable viscosity on the channel flow of water-based nanofluid under the influence of convective heat exchange with the ambient surroundings in the presence of non-uniform heat sources. Such flows are very important in engine cooling, solar water heating, cooling of electronics, cooling of transformer oil, improving diesel generator efficiency, cooling of heat exchanging devices, improving heat-transfer efficiency of chillers, domestic refrigerator and freezers, cooling in machining and in nuclear reactor. In the following sections, the problem is formulated, numerically analysed, and solved. Pertinent results are displayed graphically and discussed.

2. Formulation of the Problem

Consider the steady flow of an electrically conducting, viscous fluid through a porous medium in a vertical channel by flat walls. A uniform magnetic field of strength Ho is applied normal to the walls. Assuming the magnetic Reynolds number to be small we neglect the induced magnetic field in comparison to the applied field. The left wall is maintained at constant temperature T_1 and the right wall is at constant temperature T_0, and concentration C_1, C_0. We consider a rectangular Cartesian coordinate system O(x,y) with x-axis along the walls and y-axis normal to the walls. The walls are taken at y= ± 1 (Fig.1).

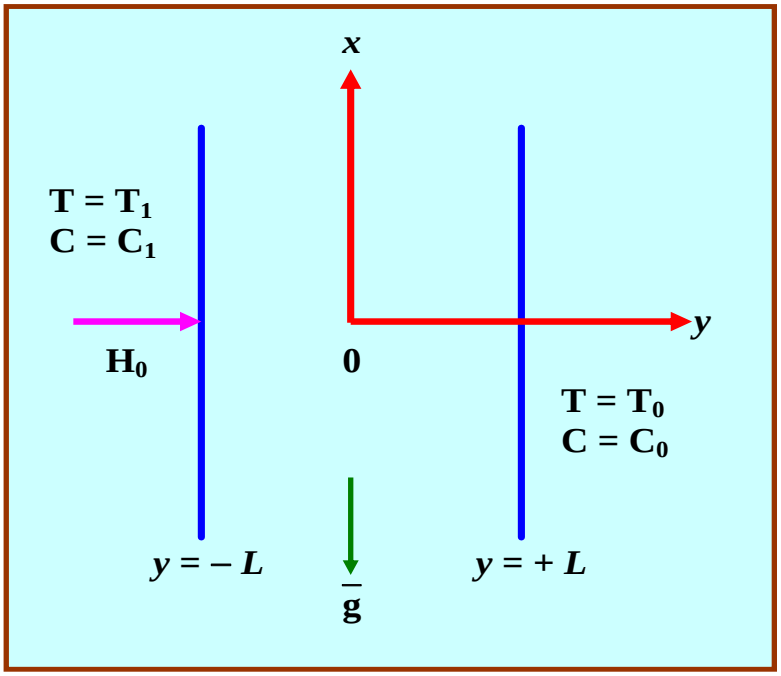

Fig.1. Schematic diagram of the problem under consideration

The boundary layer equations of flow heat and mass transfer under Boussinesq approximation and following Buongiorno model[5] are:

Equation of Continuity

$$\frac{\partial u}{\partial x} = 0 \qquad (1)$$

Momentum equation

$$0 = -\frac{\partial p}{\partial x} + \frac{\partial}{\partial y}(\mu_f(T)\frac{\partial u}{\partial y}) - \frac{\sigma B_o^2}{\rho_f}u - \frac{\mu_f(T)}{k_p}u + g[(1-C_o)\beta\rho_{f_\infty}(T-T_0) - (\rho_p - \rho_{f_\infty})(C-C_0)] \qquad (2)$$

Energy equation

$$0=\alpha_f\frac{\partial^2 T}{\partial y^2}+(\frac{\tau}{\rho C_p})(D_B\frac{\partial T}{\partial y}\frac{\partial C}{\partial y}+(\frac{D_T}{T_m})(\frac{\partial T}{\partial y})^2)+(\frac{1}{\rho C_p})(A_{11}^{'}(T_w-T_\infty)\frac{\partial f}{\partial y}+$$
$$+B_{11}^{'}(T-T_\infty)+\frac{\alpha_f\mu_f(T)}{\rho C_p}(\frac{\partial u}{\partial y})^2+\frac{\sigma B_o^2}{\rho C_p}(u^2) \quad (3)$$

Diffusion equation

$$0=D_B\frac{\partial^2 C}{\partial y^2}+(\frac{D_T}{T_m})\frac{\partial^2 T}{\partial y^2}-k_c(C-C_o)(\frac{T}{T_0})^n Exp(-\frac{E_n}{kT}) \quad (4)$$

The boundary conditions relevant to the problem are

$$u(-1)=0, T=T_1, C=C_1 \quad on\ y=-L$$
$$u(+1)=0, T=T_0, C=C_0 \quad on\ y=+L \quad (5)$$

The dynamic viscosity of the nanofluids is assumed to be temperature dependent as follows:

$$\mu_f(T)-\mu_o Exp(-m(T-T_o)) \quad (6)$$

Where μ_o is the nanofluid viscosity at the ambient temperature To. m is the viscosity variation parameter which depends on the particular fluid.

Introducing non-dimensional variables as

$$\eta=\frac{y}{L}, u'=\frac{uL}{\mu_o}, \theta=\frac{T-T_0}{T_1-T_0}, \varphi=\frac{C-C_0}{C_1-C_0}, p'=\frac{pL^2}{\mu_o^2} \quad (7)$$

The equations (2-4) reduce to

$$\frac{d^2u}{dy^2}-B\frac{du}{dy}\frac{d\theta}{dy}-Ku+e^{b\theta}(A-M^2u+Gr(\theta-N\phi))=0 \quad (8)$$

$$\frac{d^2\theta}{dy^2}+Nb\frac{d\theta}{dy}\frac{d\varphi}{dy}+Nt(\frac{d\theta}{dy})^2+A_{11}f''+B_{11}\theta+Ec(e^{-B\theta})(\frac{d^2u}{dy^2})^2+EcM^2(\frac{du}{dy})^2=0 \quad (9)$$

$$\frac{d^2\varphi}{dy^2}+(\frac{Nt}{Nb})\frac{d^2\theta}{dy^2}-\gamma Sc\phi(1+n\delta\theta)Exp(-\frac{E_1}{1+\delta\theta})=0 \quad (10)$$

The corresponding boundary conditions are

$$u(-1)=0, \theta(-1)=1, \varphi(-1)=1$$
$$u(+1)=0, \theta(+1)=0, \varphi(+1)=0 \quad (11)$$

Where

$$Gr = \frac{\beta_T g(T_1 - T_0)L^3}{\mu_o^2}, M = \frac{\sigma B_o^2 L^2}{\mu_o}, K = \frac{L^2}{k_p}, N = \frac{\beta_C (C_1 - C_0)}{\beta_T (T_1 - T_0)}, B = m(T_1 - T_0),$$

$$Nb = \frac{\tau D_B (C_1 - C_0)}{\alpha_f}, Nt = \frac{\tau D_T (T_1 - T_0)}{\alpha_f}, \mathrm{A}_{11} = \frac{L^2 A_{11}^{'}}{\rho C_p}, \mathrm{B}_{11} = \frac{L^2 B_{11}^{'}}{\rho C_p} \theta_w = \frac{T_1}{T_o}, \delta = \theta_w - 1, E_1 = \frac{E_n}{KT_0},$$

$$Ec = \frac{\mu_0}{k_f L^2 (T_1 - T_0)}. Sc = \frac{\nu}{D_B}$$

Are the Grashof number, magnetic parameter, Darcy parameter, buoyancy ratio, viscous parameter, Brownian motion parameter, thermophoresis parameter, space dependent heat source parameter, temperature dependent heat source parameter, temperature difference parameter, activation energy parameter, Eckert number, Schmidt parameter and Convective heat transfer constant.

3. Numerical Analysis

The coupled non-linear ODEs (8)-(10) along with the corresponding Bc's (11) are solved by employing the RKF algorithm with Mathematica programming. The numerical solutions are carried out by choosing the step size $\Delta\eta$=0.001.

(i)The coupled non-linear system of equations was transformed into a set of first order Des.

$$f = f_1, f' = f_2, f'' = f_3, \theta = f_4, \theta' = f_5, \phi = f_6, \phi' = f_7$$

(ii)The system of first order Des are

$$f''' = (Bf_2 f_4 + Kf_1) - e^{Bf_4}(A - M^2 f_1 + Gr(f_4 - Nf_6)) \quad (12)$$

$$\theta'' = -(Nbf_5 f_7 + Ntf_5^2 + Ece^{-Bf_4} f_3^2 + A_{11} f_2 + \mathrm{B}_{11} \mathrm{f}_4) \quad (13)$$

$$\varphi'' = -(\frac{Nt}{Nb})(f_4 f_6 + Nt^2 f_4^2 + Ece^{-Bf_4} f_3^2 + EcM^2 f_2^2 + \gamma Scf_6(1 + n\delta f_4)e^{-E1/(1+\delta f_4)}) \quad (14)$$

The boundary conditions are

$$f_1(\pm 1) = 0, f_4(-1) = 1, f_5(+1) = 0, f_6(-1) = 1, f_6(+1) = 0 \quad (15)$$

(iii) Suitable guess values are chosen for unknown required Bcs.

(iv) RKF technique with shooting method is utilized for step by step integration with the assistance of Mathematica software.

4. Skin Friction Nusselt and Sherwood Number

The quantities of physical interest in this analysis are the skin friction, coefficient Cf, local Nusselt number(Nu), local Sherwood number(Sh) which are defined as

$$C_f = \frac{2\tau_w}{\rho u_w^2}, Nu = \frac{xq_w}{\alpha_f (T_1 - T_o)}, Sh = \frac{xm_w}{D_B (C_1 - C_o)} \tag{16}$$

where

$$\tau_w = \mu(\frac{\partial u}{\partial y})_{\eta=\pm1}, q_w = k_{nf}(\frac{\partial T}{\partial y})_{\eta=\pm1}, m_w = D_B(\frac{\partial C}{\partial y})_{\eta=\pm1} \tag{17}$$

Substituting equation (17) into equation (16), we get

$$Cf = e^{-B\theta}\frac{\partial u}{\partial y})_{\eta=\pm1}, Nu = -(\frac{\partial \theta}{\partial y})_{\eta=\pm1}, Sh = -(\frac{\partial \phi}{\partial y})_{\eta=\pm1} \tag{18}$$

5. Comparison

In the absence of dissipation (Eckert number (Ec=0)) the results are good agreement with Satya Narayana and Ramakrishna et al.[20]

Table 1: Comparison.

Parameters		Satyanrayana & Ramakrishna[20]		Present Results		Satyanrayana & Ramakrishna[20]		Present Results	
		η = –1				η = +1			
		Nu(-1)	Sh(-1)	Nu(-1)	Sh(-1)	Nu(+1)	Sh(+1)	Nu(+1)	Sh(+1)
B	0.3	0.14162	0.92367	**0.14172**	**0.92366**	0.85706	0.11955	**0.85714**	**0.11957**
	0.5	0.1276	0.93711	**0.1271**	**0.93707**	0.87008	0.10711	**0.87011**	**0.10712**
	0.7	0.1147	0.94947	**0.1153**	**0.94952**	0.88172	0.09597	**0.88175**	**0.09587**
E1	0.1	0.14162	0.92367	**0.14158**	**0.92366**	0.85706	0.11955	**0.85709**	**0.11954**
	0.3	0.14171	0.91271	**0.14176**	**0.91279**	0.85761	0.12292	**0.85769**	**0.12295**
	0.5	0.14177	0.90431	**0.14179**	**0.90429**	0.85802	0.12551	**0.85807**	**0.12563**
δ	0.2	0.2602	0.82244	**0.2614**	**0.82251**	0.71976	0.24821	**0.71980**	**0.24829**
	0.4	0.14183	0.94707	**0.14195**	**0.94714**	0.85565	0.11422	**0.85569**	**0.11424**
	0.6	0.14177	0.95827	**0.14168**	**0.95833**	0.86517	0.11655	**0.86521**	**0.11659**
Nb	0.2	0.14162	0.92367	**0.14163**	**0.92369**	0.85706	0.11955	**0.85709**	**0.11961**
	0.3	0.11926	0.83461	**0.11925**	**0.83469**	0.90232	0.19255	**0.90233**	**0.19257**
	0.4	0.09203	0.77547	**0.09211**	**0.77542**	0.9638	0.23907	**0.9641**	**0.23911**
Nt	0.1	0.24231	0.93412	**0.24228**	**0.93411**	0.74947	0.11932	**0.74951**	**0.11932**
	0.3	0.08346	1.41712	**0.08345**	**1.41711**	0.98995	-0.529	**0.99001**	**-0.5295**
	0.5	0.05217	1.76395	**0.05219**	**1.76401**	1.07719	-1.0786	**1.07721**	**-1.0789**

6. RESULTS AND DISCUSSION

The aim of this analysis is to study the combined influence of dissipation, Activation energy, Brownian motion and thermophoresis on convective heat transfer flow of nanofluid confined

in vertical channel in the presence of irregular heat source. The effect of pertinent parameters on flow characteristics have been studied on solving the coupled non-linear governing equations by Runge-Kutta Shooting method.

Figs.2a-2c demonstrate the effect of Grashof number(G) and magnetic parameter(M) on the velocity, temperature and nanoparticle concentration From the profiles we find that the velocity, temperature upsurge while the nanoparticle concentration retards in the flow region with increasing values of G. This shows that an increase in G grows the thickness of the momentum, thermal boundary layers and decays solutal layer thickness. With higher the strength of the Lorentz force the velocity, nanoparticle concentration decrease and temperature rises. Physically, a retarding force or drag force (Lorentz force) is generated due to the presence of a magnetic force. On the other hand, the heat measure enhances and the mass of the fluid are depicted in figures 2b&c.

The effect of viscosity parameter(B) and buoyancy ratio(Nr) on flow variables can be seen from figs.3a-3c. Higher the viscosity parameter(B) larger the velocity, temperature and smaller the nanoparticle concentration in the flow region. When the molecular buoyancy force dominates over the thermal buoyancy force the velocity, temperature experience enhancement while nanoparticle concentration depreciates when the buoyancy forces are in the same direction.

Lesser the molecular diffusivity/higher the dissipative force(Ec) larger the velocity, temperature and smaller the nanoparticle concentration (figs.4a-4c). This may be attributed to the fact that increase in Sc and Ec leads to a growth in momentum and thermal boundary thickness while solutal layer becomes thinner in the flow region.

Figs.5a-5c exhibits the effect of chemical reaction parameter (γ) of θ and C. From the profiles we find that the velocity, temperature increase and nanopaticle concentration depreciate in both degenerating/generating chemical reaction cases. This may be attributed to the fact that an increase in $\gamma>0$ leads to growth of momentum, thermal and decays solual boundary layers.

Figs.6a-6c exhibit the effect of temperature relative parameter(δ) and activation energy parameter(E1) on flow variables. Increasing activation energy(E1) leads to a fall in velocity and rise in temperature and nanoparticle concentration in the flow region. The effect of temperature difference parameter (δ) is to enhance velocity, temperature and depreciates

nanoparticle concentration. This is due to the fact that an increase in temperature relative parameter (δ) leads to thickening of the momentum and thermal boundary layers and thinning of the solutal boundary layer.

The effect of space dependent/temperature dependent heat sources (A11,B11) on flow variables can be seen from figs.7a-7c and 8a-8c. From the profiles we find that the velocity, temperature enhance with rising values of space dependent/generating heat source (A11>0,B11>0) and reduces with heat sink (A11<0,B11<0) (fig.7a,b&8a,b). The nanoparticle concentration (ϕ) exhibits an opposite effect with space/temperature dependent heat source (figs.7c&8c).

Figs.9a-9c represent the effect of Brownian motion (Nb) and thermophoresis parameter(Nt) on flow variables. A rise in Nb and Nt leads to a growth in velocity, temperature while nanoparticle concentration grows with Nb and decays with Nt. Physically, thermophoretic force creates a rise in the flow region. Consequently, as Nt increases the thickness of the momentum, thermal become layers become thicker and solutal layer becomes thinner (figs.9a-9c).

Figs.10a-10c represent the effect of thermal diffusivity and index number(n) on velocity, temperature and nanoparticle concentration. From the profiles we find that the velocity, temperature enhance while nanoparticle concentration depreciates with rising values of Prandtl number and index number.

The skin friction factor (Cf), Nusselt (Nu) and Sherwood number (Sh)at the walls $\eta = \pm 1$ are exhibited in table.2. From the tabular values we observe that the skin friction(Cf) grows at both the walls with increasing values of G, Ec,Sc,Nt,δ, γ and Pr. Lesser the thermal diffusivity/temperature excess ratio(δ), smaller Cf on $\eta = \pm 1$.Cf enhances with higher values of Lorentz force/index number(n),larger Cf at the left wall and smaller at the right wall. When the molecular buoyancy force dominates over the thermal buoyancy force, Cf reduces at the left wall and enhances at the right wall. Increase in space /temperature dependent heat source (A11>0, B11>0) leads to a rise in Cf at both the walls, while it enhances at the left wall and reduces at the right wall with heat sink(A11<0.B11<0).Cf enhances with γ>0 and reduces with γ<0 at η=-1 while at η=+1,Cf upsurges in both degenerating/generating chemical reaction cases.

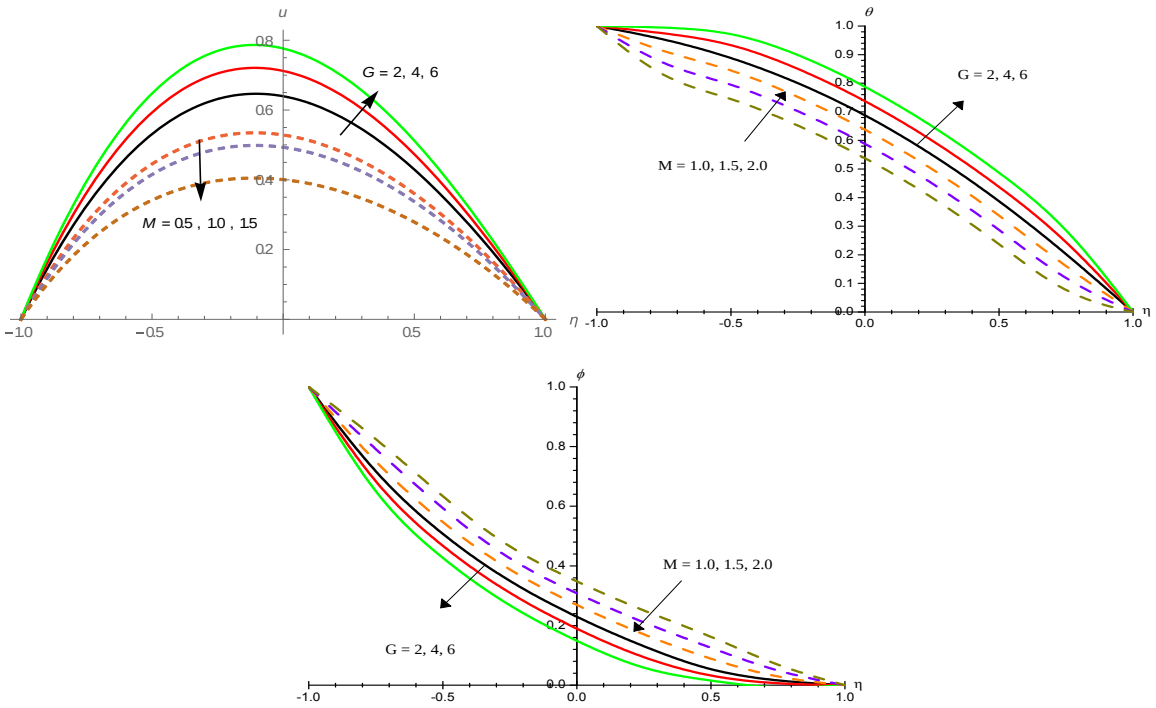

Fig. 2: Variation of [a] velocity (*u*), [b] Temperature (θ), Concentration(ϕ) with G and M.

Nr=0.2, B=0.3, Ec=0.05, Sc=0.24, γ=0.5, E1=0.1, δ=0.2, A11=0.2, B11=0.2, Nb=0.2, Nt=0.1, *n*=0.2, Pr=0.71.

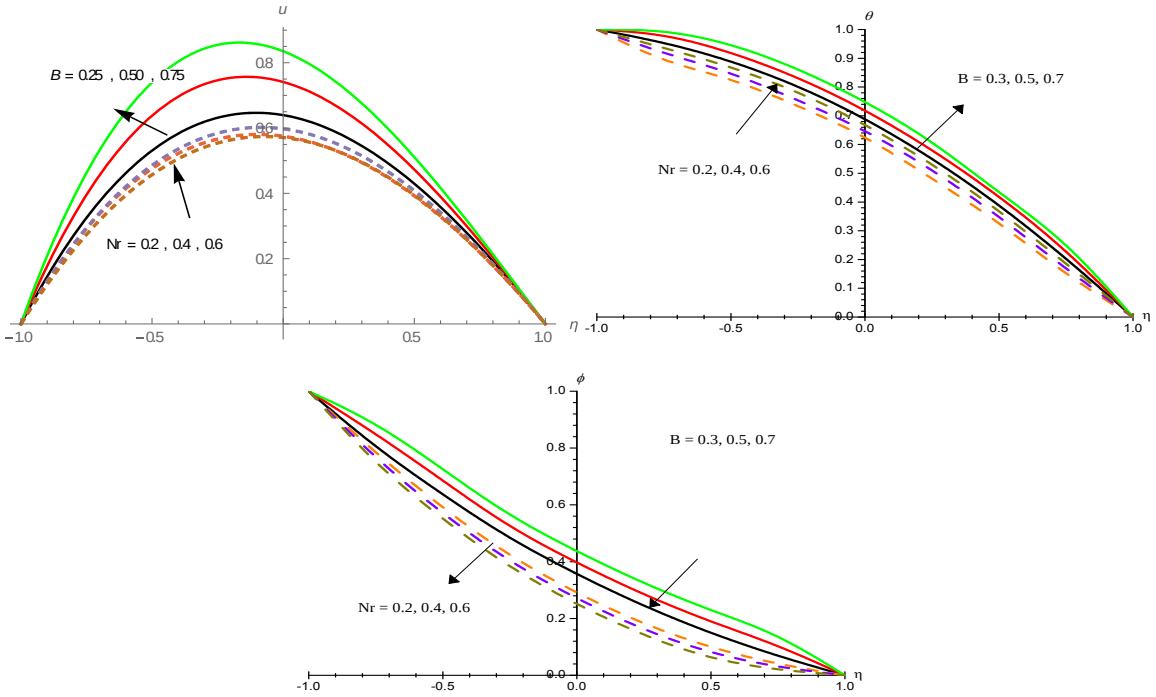

Fig. 3: Variation of [a] velocity (*u*), [b] Temperature (θ), Concentration(ϕ) with B and Nr.

G=2, M=0.5, Ec=0.05, Sc=0.24, γ=0.5, E1=0.1, δ=0.2, A11=0.2, B11=0.2, Nb=0.2, Nt=0.1, *n*=0.2, Pr=0.71

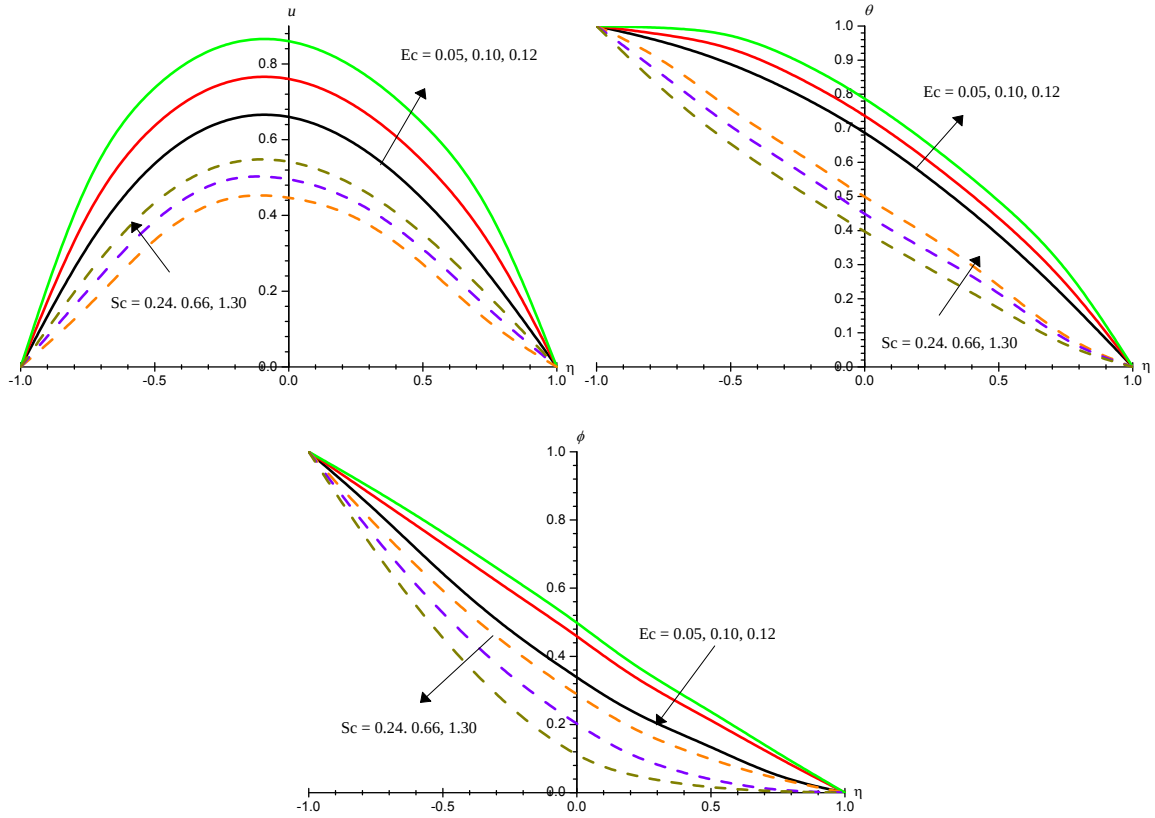

Fig. 4: Variation of [a] velocity (*u*), [b] Temperature(θ), Concentration(ϕ) with Ec and Sc.

G=2, M=0.5, Nr=0.2, B=0.3, γ=0.5, E1=0.1, δ=0.2, A11=0.2, B11=0.2, Nb=0.2, Nt=0.1, *n*=0.2, Pr=0.71

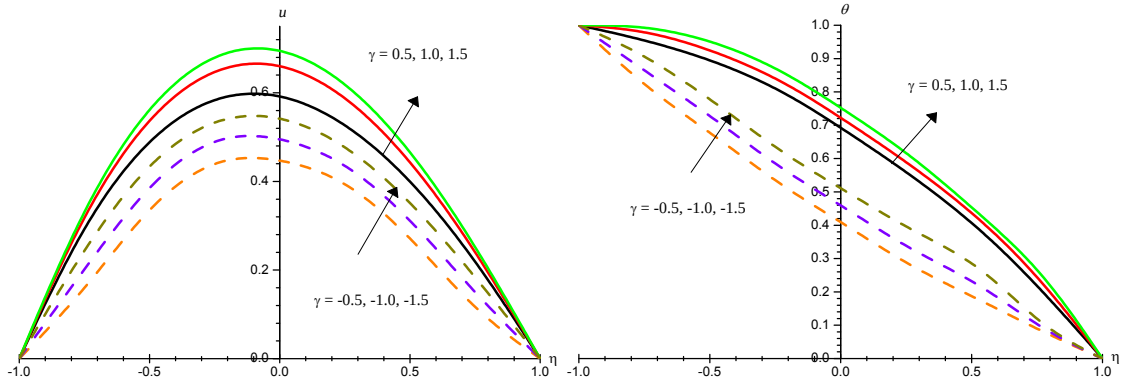

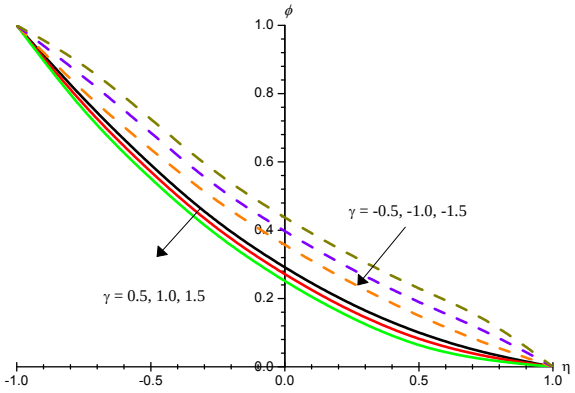

Fig. 5: Variation of [a] velocity (*u*), [b] Temperature(θ), Concentration(ϕ) with γ.

G=2, M=0.5, Nr=0.2, B=0.3, Ec=0.05, Sc=0.24, E1=0.1, δ=0.2, A11=0.2, B11=0.2, Nb=0.2, Nt=0.1, *n*=0.2, Pr=0.71.

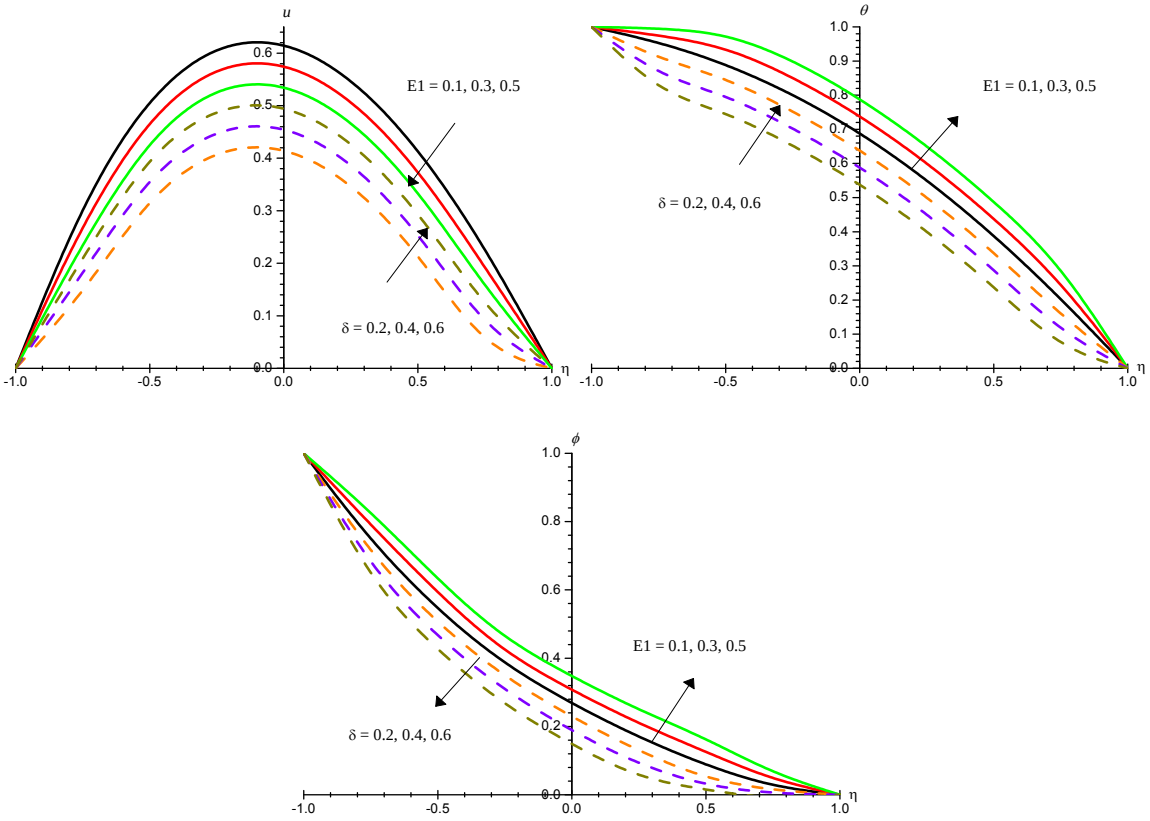

Fig. 6: Variation of [a] velocity(*u*), [b] Temperature(θ), Concentration(ϕ) with E1 & δ.

G=2, M=0.5, Nr=0.2, B=0.3, Ec=0.05, Sc=0.24, γ=0.5, A11=0.2, B11=0.2, Nb=0.2, Nt=0.1, *n*=0.2, Pr=0.71

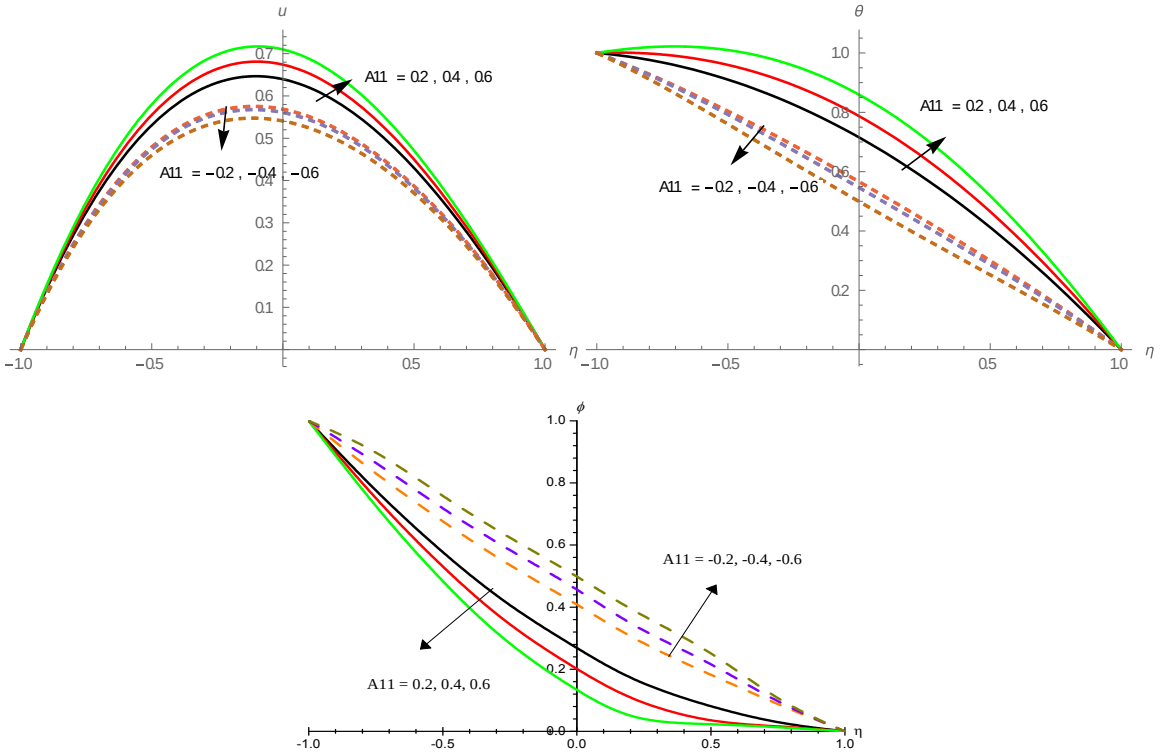

Fig. 7: Variation of [a] velocity(*u*), [b] Temperature(θ), Concentration(ϕ) with A11.

G=2, M=0.5, Nr=0.2, B=0.3, Ec=0.05, Sc=0.24, γ=0.5, E1=0.1, δ=0.2, B11=0.2, Nb=0.2, Nt=0.1, *n*=0.2, Pr=0.71

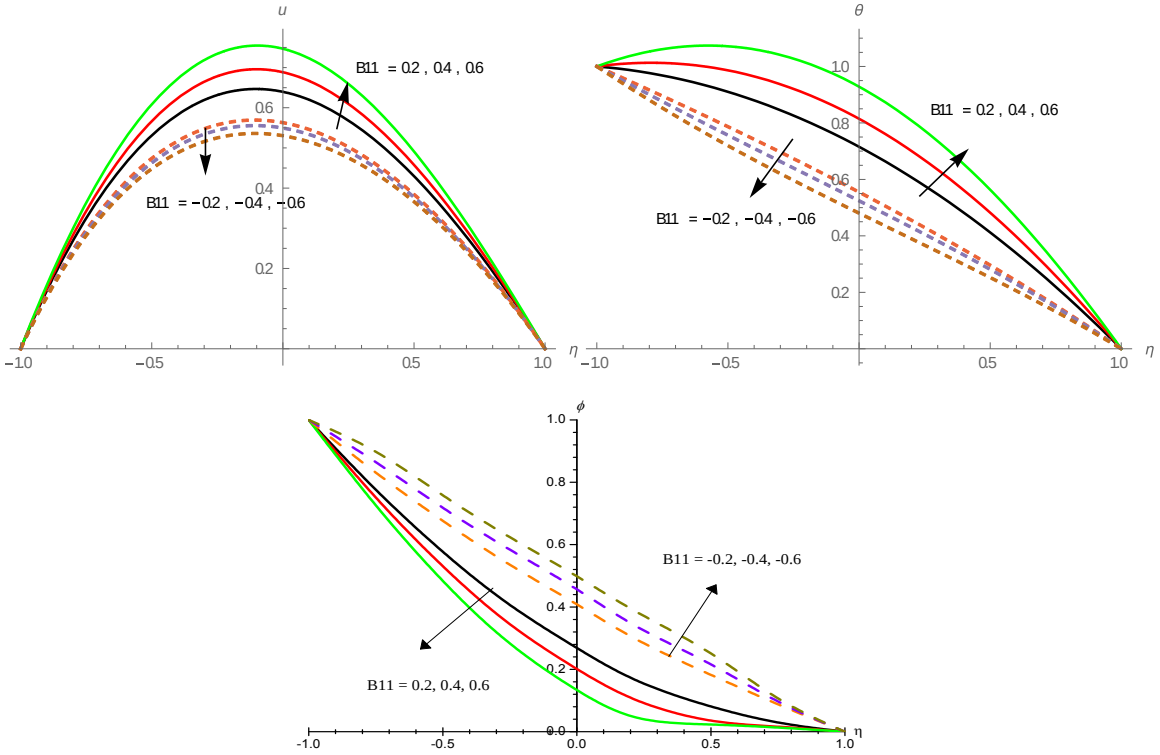

Fig. 8: Variation of [a] velocity(*u*), [b] Temperature(θ), Concentration(ϕ) with B11.

G=2, M=0.5, Nr=0.2, B=0.3, Ec=0.05, Sc=0.24, γ=0.5, E1=0.1, δ=0.2, A11=0.2, Nb=0.2, Nt=0.1, *n*=0.2, Pr=0.71.

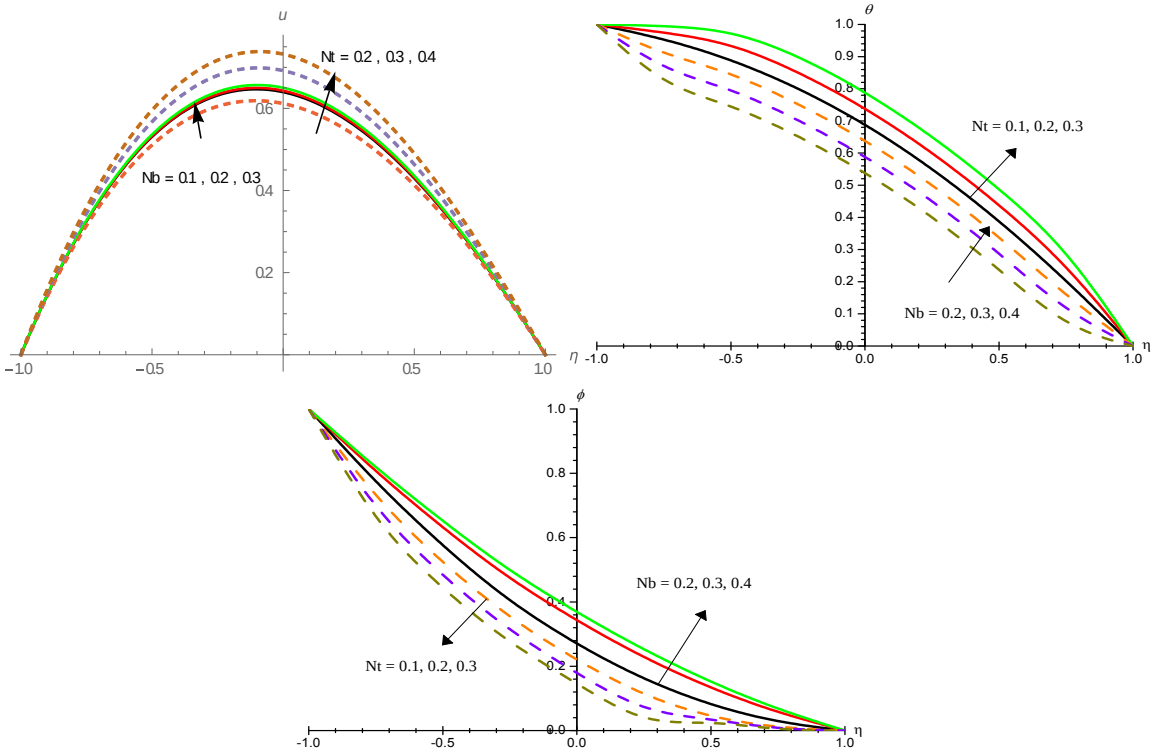

Fig.9: Variation of [a] velocity(*u*), [b] Temperature(θ), Concentration(ϕ) with Nb and Nt.

G=2, M=0.5, Nr=0.2, B=0.3, Ec=0.05, Sc=0.24, γ=0.5, E1=0.1, δ=0.2, A11=0.2, B11=0.2, *n*=0.2, Pr=0.71.

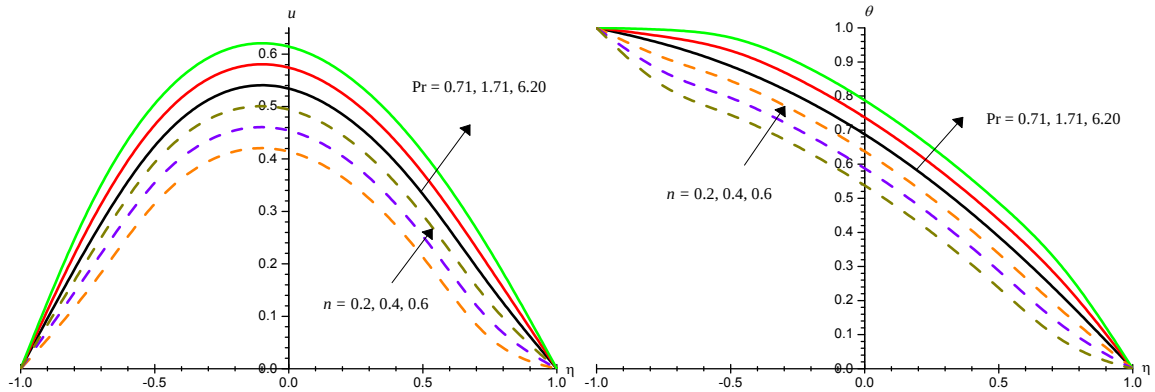

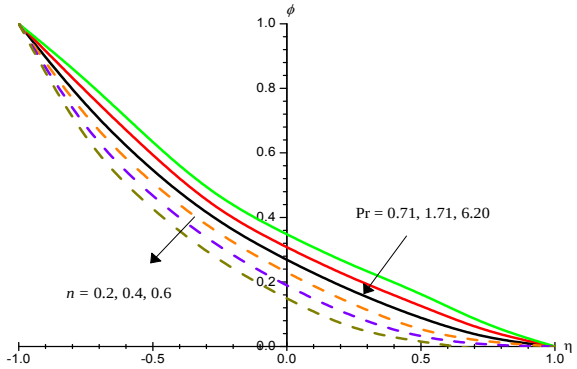

Fig. 11: Variation of [a] velocity(*u*), [b] Temperature(θ), Concentration(ϕ) with *n* and Pr.

G=2, M=0.5, Nr=0.2, B=0.3, Ec=0.05, Sc=0.24, γ=0.5, E1=0.1, δ=0.2, A11=0.2, B11=0.2, Nb=0.2, Nt=0.1.

The rate of heat transfer(Nu) depreciates at η=-1 and enhances at η=+1 with rising values of G, B, Nr, Sc and n. Nu enhances at the let wall and reduces at the right wall with rising values of M, Nu decays with δ, Nb, Nt and Pr at both the walls. Nusselt number reduces at both walls in the degenerating chemical reaction case while in the generating case, Nu reduces at the left wall and enhances at the right wall. The rate of heat transfer enhances with rise in A11>0,B11>0 at the left wall(η=-1). At the right wall(η=+1)Nu enhances with γ>0 and reduces with γ<0.An increasing activation energy (E1)enhances Nu while it reduces with δ at both the walls.

The rate of mass transfer(Sh)enhances at η=-1 and reduces at η=+1,with increasing values of, G,Nr,Ec,Sc,δ and Pr. An opposite is noticed in Sh with rise in M,E1,Sh reduces with Nb and enhances with Nt at $\eta = \pm 1$.Also Sh enhances at η=-1 and reduces at η=+1with γ>0 while for γ<0,Sh enhances at both the walls. Sh enhances at the left wall and reduces at the right wall with A11>0 while an opposite effect is noticed in Sh with A11<0.Sh reduces at η=-1 with B11>0 and enhances with B11<0.At the right wall, Sh grows with B11>0 & B11<0. In addition, AE(E1) plays an important role in increasing the local heat transfer coefficient. Generally, AE is the minimum amount of energy that is required for a chemical reaction to stimulates atoms or molecules in the reaction. There should a considerable number of atoms whose AE is less than or equal to translational energy in a chemical reaction, hence in many engineering applications, AE may be considered as a better coolant.

Table 2: Skin-Friction (Cfx) and Nusslet(Nu) and Sherwood(Sh) Numbers at η = ± 1.

Parameters		η = –1			η = +1		
		Cfx(-1)	Nu(-1)	Sh(-1)	Cfx(+1)	Nu(+1)	Sh(+1)
G	2	1.50679	0.24686	0.88942	-0.9823	0.73108	0.21544
	4	2.13407	0.19167	0.94147	-1.2554	0.78258	0.16713
	6	2.84262	0.11075	1.01787	-1.5876	0.85829	0.09595
M	0.5	1.37382	0.22878	0.90611	-0.8957	0.75008	0.19783
	1.0	1.2512	0.26374	0.87344	-0.8145	0.71317	0.23241
	1.5	1.3847	0.27486	0.86298	-0.7036	0.70136	0.24354
B	0.25	1.5575	0.07453	0.98147	-1.0186	0.93152	0.04905
	0.50	1.91161	0.04807	1.00699	-1.0508	0.95859	0.02291
	0.75	2.25107	0.02293	1.03127	-1.0747	0.98384	-0.01145
Nr	0.2	1.40987	0.22631	0.83508	-0.9593	0.75736	0.21763
	0.4	1.38996	0.16128	0.90518	-0.9805	0.86731	0.06278
	0.6	1.28225	0.10146	0.95529	-0.9994	0.90862	0.07125
A11	0.2	1.55732	0.07453	0.98147	-1.0186	0.9315	0.04905
	0.4	1.59782	-0.09273	1.08407	-1.0473	1.05878	0.02352
	0.6	1.63895	-0.14043	1.18709	-1.0761	1.18696	0.01693
	-0.2	1.46533	0.32893	0.73674	-0.9556	0.64411	0.32654
	-0.4	1.45562	0.32933	0.70741	-0.9486	0.63046	0.33906
	-0.6	1.42952	0.40001	0.66966	-0.9301	0.54729	0.41922
B11	0.2	1.55782	0.07453	0.98147	-1.0186	0.93153	0.04905
	0.4	1.55641	0.07462	0.97205	-1.0585	1.09668	0.10963
	0.6	1.55596	0.07475	0.96483	-1.1041	1.29014	0.29557
	-0.2	1.50472	0.21987	0.84512	-0.9514	0.63935	0.33068
	-0.4	1.55031	0.06547	0.98726	-0.9396	0.62513	0.34319
	-0.6	1.55047	0.07544	0.99022	-0.9222	0.55791	0.40766
Nb	0.1	1.55744	0.07453	0.98147	1.55755	0.07453	0.98147
	0.2	1.55464	0.03797	0.82297	1.55464	0.03797	0.82297
	0.3	1.54978	0.02886	0.76527	1.55278	0.01864	0.76527
Nt	0.2	1.52314	0.20085	0.98476	1.52314	0.20085	0.98476
	0.3	1.63015	0.01463	1.56261	1.63015	0.01759	1.56261
	0.5	1.68765	0.00973	1.97404	1.68765	0.01274	1.97404
E1	0.1	1.55743	0.07453	0.98147	-1.0186	0.9315	0.04905
	0.3	1.55641	0.07462	0.97205	-1.0182	0.93192	0.05187
	0.5	1.54996	0.07475	0.96483	-1.0176	0.93225	0.05404
δ	0.2	1.50472	0.21987	0.84514	-0.9832	0.96246	0.21153
	0.4	1.55031	0.09547	0.98726	-1.0154	0.93018	0.04842
	0.6	1.55047	0.07544	0.99022	-1.0165	0.93006	0.04775
Ec	0.05	1.55742	0.07453	0.98147	-1.0186	0.9315	0.04305
	0.10	1.57431	-0.08434	1.05829	-1.0309	1.01876	0.03615
	0.12	1.59135	-0.09951	1.13323	-1.0431	1.10415	0.01956
Sc	0.24	1.51022	0.21864	0.92897	-0.9863	1.20038	0.18186
	0.66	1.55815	0.07427	1.12117	-1.0195	0.92455	0.09236
	1.30	1.56165	0.07079	1.18361	-1.0212	0.93213	0.04246
γ	0.5	1.55744	0.07453	0.98147	-1.0186	0.93152	0.04905
	1.0	1.55868	0.07426	1.00877	-1.0194	0.93031	0.04125
	1.5	1.55998	0.07406	1.03017	-1.0201	0.92942	0.03531

	-0.5	1.49897	0.22117	1.05984	-0.9799	0.76466	0.24331
	-1.0	1.54464	0.09945	0.89456	-1.0123	0.93437	0.09918
	-1.5	1.53268	0.07672	0.86443	-1.0213	0.93583	0.08589
n	0.2	1.52131	0.15913	0.97247	-0.9943	0.82339	0.12795
	0.4	1.52235	0.13974	0.99166	-0.9951	0.84232	0.10932
	0.6	1.53401	0.08198	1.04667	-1.0034	0.90239	0.05207
Pr	0.71	1.50679	0.24686	0.88942	-0.9823	0.73108	0.21544
	1.71	1.50791	0.24663	0.90836	-0.9829	0.73074	0.21045
	6.20	1.50901	0.24641	0.92708	-0.9835	0.73041	0.20558

7. CONCLUSION

The effect of dissipation, irregular heat sources, variable viscosity and activation energy on flow characteristics in a vertical channel is analysed. The conclusions of this analysis are

1. An increase in viscosity parameter(B) enhances the velocity, temperature and reduces nanoparticle concentration The skin friction, Sherwood number grow, Nusselt number decays with B at the left wall and an opposite effect is observed at the right wall.
2. Temperature and nanoparticle concentration grow and velocity augments with increase in E1. Increase in δ grows the velocity, temperature and reduces nanoparticle concentration. Cf reduces and enhances E1 and decays with δ. Nu enhances at both the walls with E1. Cf reduces with E1 and enhances with δ Nu increases with E1 and reduces with δ at $\eta = \pm 1$.
3. Lesser molecular diffusivity/higher the dissipative force, larger velocity and temperature, smaller Concentration. Cf Sh grow, Nu decay with Sc.Cf, Nu grow with Ec at. $\eta = \pm 1$.
4. Velocity, temperature enhance and nanoparticle concentration reduces in both degenerating/generating chemical reaction cases. Nu reduces at both walls with γ>0 while Sh reduces at the right wall.
5. The velocity, temperature increase, nanoparticle concentration reduces with increase in the strength of the space /temperature dependent heat source (A11>0,B11>0). Nusselt number grows with A11 and B 11.
6. Brownian motion and thermophoresis exhibit an increasing tendency in velocity, temperature. Rise in Nb decays Nu and Sh while increase in Nt decays Nu and grows Sh at both the walls.

8. REFERENCES

1. Abo-Eldahab E. M. Abd El Aziz M. Hall and ion-slip effect on MHD free convective heat generating flow past a semi-infinite vertical flat plate Phs. Scripta, 2000; 61: 344.
2. Abu-Nada E., Application of nanofluids for heat transfer enhancement of separated flows encountered in a backward facing step, Int. J. Heat Fluid Flow, 2008; 29: 242–249.

3. Al-Nimir, M.A., Haddad, O. H: Fully developed free convection in open-ended vertical channels partially filled with porous material, Journal Porous Media, 1999; 2: 179-189.
4. Barletta A and Pulvirenti B Forced convection with slug flow and viscous dissipation in a rectangular duct, *Int. J. Heat and Mass Transfer*, 2000; 43(5): 725-740.
5. Buongiorno J., Convective transport in nanofluids, J. Heat Transf, 2006; 128: 240–250.
6. Cebeci, T, Khattab, A. A and LaMont, R: Combined natural and forced convection in a vertical ducts, in: Proc. 7th Int. Heat Transfer Conf., 1982; 3: 419-424.
7. Choi S.U.S., Enhancing thermal conductivity of fluids with nanoparticles, in: Proc. ASME Int. Mech. Eng. Congress and Exposition, ASME, San Francisco, USA, 1995: 99–105, FED 231/MD 66.
8. Choi S.U.S., Zhang Z.G., Yu W., Lockwood F.E., Grulke E.A., Anomalously thermal conductivity enhancement in nanotube suspensions, Appl. Phys. Lett, 2001; 79(2): 2252–2254.
9. Ghebhart B and Mollendorf J. Viscous dissipation in external natural convection flows, *Journal of Fluid Mechanics*, 1969; 38: 97-107.
10. Gill, W.N. and Del Casal, A: A theoretical investigation of natural convection effects in forced horizontal flows, AICHE J, 1962; 8: 513-518.
11. Greif, R., Habib, I.S and Lin, J.C: Laminar convection of a radiating gas in a vertical channel, J. Fluid. Mech., V., 1971; 46: 513.
12. Hwang K.S., Lee J.-H., Jang S.P., Buoyancy-driven heat transfer of water-based Al2O3nanofluids in a rectangular cavity, Int. J. Heat Mass Transf, 2007; 50: 4003–4010.
13. Ibrahim W., Makinde O.D., The effect of double stratification on boundary-layer flow and heat transfer of nanofluid over a vertical plate, Comput. Fluids, 2013; 86: 433–441.
14. Makinde O.D., Analysis of Sakiadis flow of nanofluids with viscous dissipation and Newtonian heating, Appl. Math. Mech, 2012; 33(12): 1545–1554.
15. Mutuku-Njane W.N., Makinde O.D., MHD nanofluid flow over a permeable vertical plate with convective heating, J. Comput. Theor. Nanosci, 2014; 11(3): 667–675.
16. Nield D.A., Kuznetsov A.V., The Cheng–Minkowycz problem for natural convective boundary-layer flow in a porous medium saturated by a nanofluid, Int. J. Heat Mass Transf, 2009; 52: 5792–5795.
17. Olanrewaju M., Makinde O.D., On boundary layer stagnation point flow of a nanofluid over a permeable flat surface with Newtonian heating, Chem. Eng. Commun, 2013; 200(6): 836–852.

18. Ostrach, S: Combined natural and forced convection laminar flow and heat transfer of fluid with and without heat sources in channels with linearly varying wall temperature, NACA TN, 1954; 3141.
19. Oztop H.F., Abu-Nada E., Numerical study of natural convection in partially heated rectangular enclosures filled with nanofluids, Int. J. Heat Fluid Flow, 2008; 29: 1326–1336.
20. Satya Narayana K and Ramakrishna G N Efect of variable viscosity, activation energy and irregular heat sources on convective heat and mass transfer flow of nanofluid in a channel with brownian motion and thermophoresis, *World Journal of Engineering Research and Technology* (JERT) *wjert, 2023; 9(2): XX-XX*, ISSN 2454-695X, SJIF Impact Factor: 5.924, www.wjert.org
21. Tiwari R.K., Das M.K., Heat transfer augmentation in a two-sided lid-driven differentially heated square cavity utilizing nanofluids, Int. J. Heat Mass Transf, 2007; 50: 2002–2018.
22. Vajravelu, K and Hadjinicolaou, A. Heat transfer in a viscous fluid over a stretching sheet with viscous dissipation and internal heat generation, *Int. Commun Heat Mass Transfer*, 1993; 20(3): 417-430.
23. Wang X.Q., Mujumdar A.S., Heat transfer characteristics of nanofluids: a review, Int. J. Therm. Sci., 2007; 46: 1–19.